SAXS Analysis of the Order−Disorder Transition and the Interaction Parameter of Polystyrene-*block*-poly(methyl methacrylate)

Yue Zhao,[†,‡] Easan Sivaniah,[§] and Takeji Hashimoto*[,†,‡]

Advanced Science Research Center (ASRC), Japan Atomic Energy Agency (JAEA), Tokai-mura, Ibaraki 319-1195, Japan; Department of Polymer Chemistry, Graduate School of Engineering, Kyoto University, Kyoto 615-8510, Japan; and Biological and Soft Sciences Sector, Department of Physics, Cavendish Laboratory, Cambridge University, Cambridge CB3 0HE, England

Received June 10, 2008
Revised Manuscript Received August 28, 2008

Introduction

In this Note, we report the discontinuous change of the scattering parameters with temperature (T) across the order−disorder transition (ODT) temperature (T_{ODT}) for the nondeuterated polystyrene-*block*-poly(methyl methacrylate) (PS-*b*-PMMA) block copolymer (BCP) system. This discontinuous change has not been reported so far for PS-*b*-PMMA though it is commonly observed for other BCPs such as PS-*block*-polyisoprene and PS-*block*-polybutadiene. We also observed that the Flory−Huggins interaction parameter, χ, between polystyrene (PS) and poly(methyl methacrylate) (PMMA) is slightly larger compared to deuterated samples, having similar molecular weight and compositions.[1,2] This implies that deuteration of either PS or PMMA or both blocks appears to increase miscibility between two blocks and lowers T_{ODT}.

PS-*b*-PMMA has been studied extensively, especially with respect to the ease of manipulation of its microdomain structure within a thin film geometry; see cited reviews.[3−5] Concurrently, there has been some effort to characterize the ODT and χ between PS and PMMA, since such information is key to controlling the microphase separation and hence the physical properties of the polymers, especially the interfacial behavior.[1,2,6−16] To address specifically the χ parameter between PS and PMMA, Stühn analyzed χ for a homogeneous short chain diblock of PS-*b*-PMMA using small-angle X-ray scattering (SAXS)[17,18] Russell et al. obtained quite different χ values (to Stühn) for deuterium-labeled BCPs (of approximately twice the molecular weight), where either PS or PMMA or both blocks were deuterated, as a function of temperature by small-angle neutron scattering (SANS).[1,2]

Although all the reported scattering results for the PS-*b*-PMMA system are obtained for homogeneous BCP melt, no paper has simultaneously reported on a PS-*b*-PMMA system's ODT. As per Russell et al., the χ value of PS-*b*-PMMA is only weakly temperature dependent; thus, although the BCP working temperature window is relatively large with a lower bound of the glass transition temperature (∼100 °C) and the upper bound of ∼250 °C where the polymer thermally degrades, the corresponding molecular weight window where the ODT can be observed is remarkably small for PS-*b*-PMMA in comparison to other BCP systems.[19,20] Amundson et al., in manipulating the alignment of lamellar microstructure by an electric field, reported (without data) a T_{ODT} of 182 °C for 31K PS-*b*-PMMA and 251 °C for 37K PS-*b*-PMMA by birefringence and dynamic mechanical spectroscopy.[21] Anastasiadis et al. and Fernandez et al. employed the χ parameter when studying the PS/PMMA interfacial width in block copolymer and homopolymer thin films.[6,10] Also within a thin film geometry, Menelle et al. demonstrated a method of determining the bulk phase T_{ODT} using an extrapolation of film thickness.[14] More recently, Wang et al. found the formation of the lithium−PMMA complexes may increase χ in PS-*b*-PMMA copolymers with the result of an increase in microdomain spacing and ordering.[22]

In this work, we report the discontinuous change of the SAXS profiles of PS-*b*-PMMA with T across T_{ODT} brought about by a fluctuation-induced first-order phase transition.[23,24] We also report the χ parameters between PS and PMMA estimated by Leibler's mean-field theory[25] at $T > T_{MF}$, where T_{MF} is regarded as the crossover temperature from a mean-field disordered state to the non-mean-field, fluctuation-influenced, disordered state.[19] Combining the earlier reported data and our work, one can better clarify the temperature dependence of χ for PS-*b*-PMMA BCPs.

Experimental Section

Sample Preparations. PS-*b*-PMMAs (sample 1: $M_n = 28$K, $M_w/M_n = 1.05$, and the volume fraction of PS, $f_{PS} = 0.56$; sample 2: $M_n = 25.7$K, $M_w/M_n = 1.05$, and $f_{PS} = 0.53$) were used directly as purchased from Polymer Source Inc. The BCP powders were first dissolved in benzene with a concentration of 5.15 wt %; then the BCP films (1 mm thick) were prepared by slow evaporation of benzene at room temperature for 1 week and then in a vacuum oven for 1 week.

SAXS Measurements. SAXS profiles were measured in situ at each temperature with the SAXS apparatus described elsewhere.[26] To suppress thermal degradation as much as possible, the sample was placed in the sample chamber filled with nitrogen gas, and the temperature was controlled with an accuracy of ±0.03 °C. The profiles were desmeared for slit-height and slit-width effects and corrected for absorption, air scattering, and thermal diffuse scattering as described elsewhere.[27,28] In Figure 1, we present the temperature protocols for the series of SAXS experiments. The SAXS measurements were conducted during a cooling process that started at 230 °C for sample 1 and 220 °C for sample 2. At these temperatures,

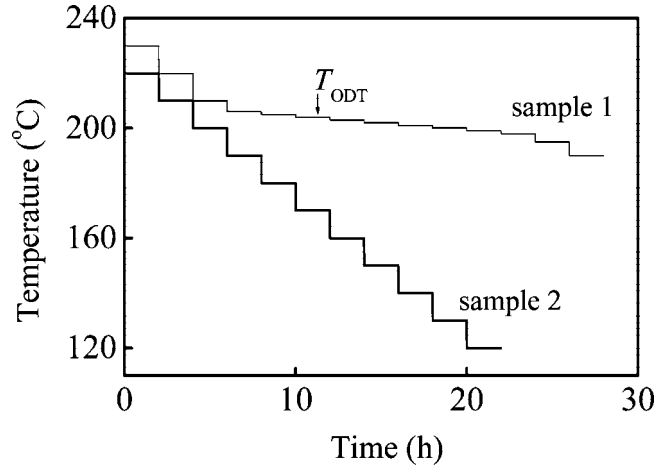

Figure 1. Thermal protocols adopted in the SAXS measurements for (a) sample 1 (PS-*b*-PMMA 28K) and (b) sample 2 (PS-*b*-PMMA 25.7K). The arrow marked by "T_{ODT}" is T_{ODT} for sample 1 (205−203 °C).

* To whom all correspondence should be addressed. Present address in ASRC and JAEA.
† ASRC and JAEA.
‡ Kyoto University.
§ Cambridge University.

10.1021/ma8013004 CCC: $40.75
Published on Web 11/24/2008

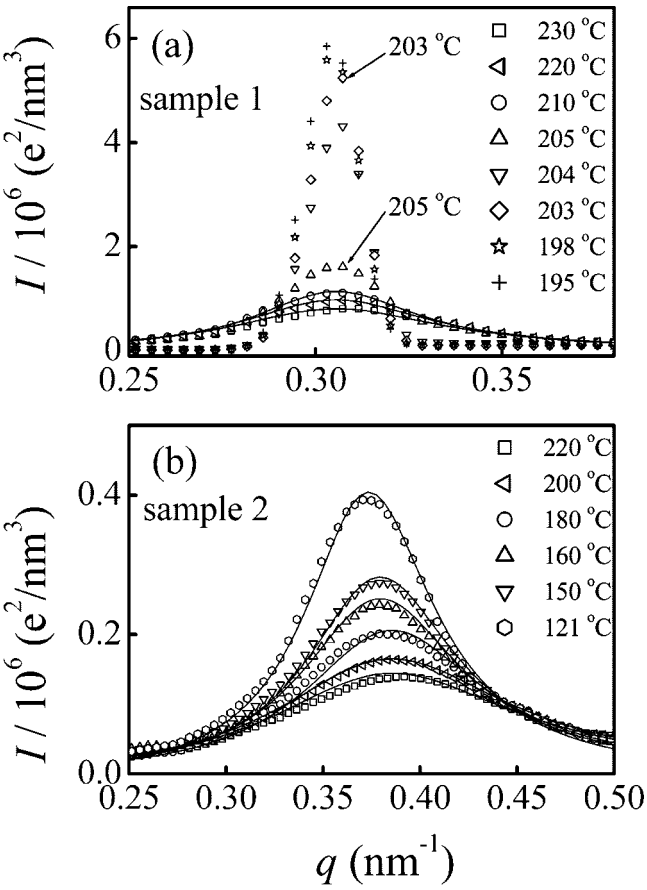

Figure 2. Temperature dependence of the SAXS profiles near the first-order peaks for (a) sample 1 and (b) sample 2. The lines in the figure show the calculated scattering profiles best-fitted with the experimental profiles by changing χ as an adjustable parameter.

both the specimens were initially in the disordered state. At each measuring temperature, the samples were held for ~60 min before the measurement with the position-sensitive detector and a measuring time of ~60 min. The T_{ODT}, determined directly by a discontinuous change of the observed SAXS profiles with T, is marked with the arrow labeled by "T_{ODT}" for sample 1. As for sample 2, no T_{ODT} was detected.

Results

Figure 2a shows desmeared SAXS profiles around the first-order scattering maximum from sample 1 taken in situ at various temperatures according to the thermal protocol shown in Figure 1. Scattering intensity is plotted against magnitude of the scattering vector q [$q = (4\pi/\lambda)\sin(\theta/2)$, where $\lambda = 0.154$ nm and θ = scattering angle]. A sharp and remarkable change of the first-order scattering profiles is clearly discerned at temperature between 205 and 203 °C. This discontinuous change of the SAXS profile enables a clear-cut determination of the T_{ODT} of sample 1. T_{ODT} thus determined is 203 °C < T_{ODT} < 205 °C. The second-order Bragg peak appears at q twice as large as the q value at the first-order scattering maximum (not shown here) at $T < T_{ODT}$, which is caused by the slightly asymmetric composition ($f_{ps} = 0.56$) and indicative of the typical lamellar morphology formed in the ordered state.

Figure 2b shows the corrected SAXS profiles from sample 2 taken in situ at various temperatures according to the thermal protocol shown in Figure 1. We observe a continuous change of the profiles near the first-order scattering maximum in terms of peak width and peak position over the temperature range covered in this work. Judging from the large peak width relative to that in the ordered state shown in Figure 2a, it is reasonable to assume that sample 2 is in the disordered state in this temperature range.

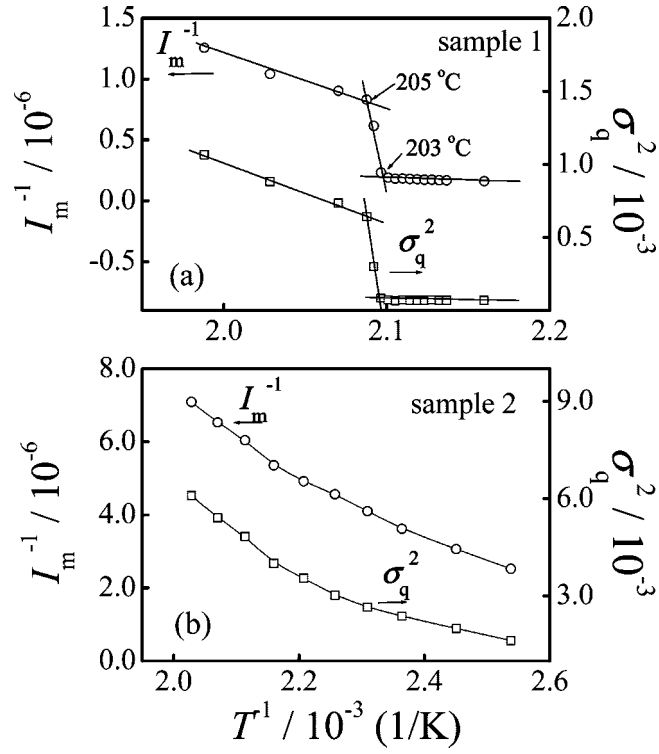

Figure 3. I_m^{-1} and σ_q^2 plotted as a function of T^{-1} for (a) sample 1 and (b) sample 2. The lines in the figure are guides to the eye.

Analysis and Discussion

Discontinuity at the ODT Temperature. A discontinuous change in the shape and height of the principal SAXS scattering peak as the temperature spans the T_{ODT} is a characteristic signature of the order−disorder transition. To quantitatively characterize ODT, the first-order peak was analyzed in terms of its maximum intensity (I_m), peak position (q_m), and half-width at half-maximum (hwhm, σ_q). Conventionally, the plot of I_m^{-1} or σ_q^2 vs T^{-1} shows a discontinuous change at T_{ODT}[18,19,29−32] as a consequence of thermal fluctuation-induced first-order transition.[23,24]

Parts a and b of Figure 3 show I_m^{-1} and σ_q^2 plotted as a function of T^{-1} for samples 1 and 2, respectively. As we expected, both I_m^{-1} and σ_q^2 have similar temperature dependence. A sharp discontinuity appears in the temperature dependence in a narrow temperature range between 205 and 203 °C for sample 1. Commonly, the curves were divided into three temperature regimes, namely, above, near, and below the transition point. In each regime, I_m^{-1} vs T^{-1} and σ_q^2 vs T^{-1} follow approximately a straight line as shown in Figure 3a. The temperature range of ODT described above was determined from the two intersections of the three lines (205 to 203 °C). As for sample 2, T_{ODT} is not clearly discerned, probably because T_{ODT} is below the observed temperature range or the glass transition temperature of the sample. The scattering data show a continuous increase of the maximum scattering intensity and a decrease of the peak width upon cooling. This is the normal behavior due to the increase of segregation force upon cooling.

Estimation of the χ Parameter. The χ parameters can be estimated by analyzing the scattering profiles from the disordered melt on the basis of Leibler's mean-field theory[25] modified

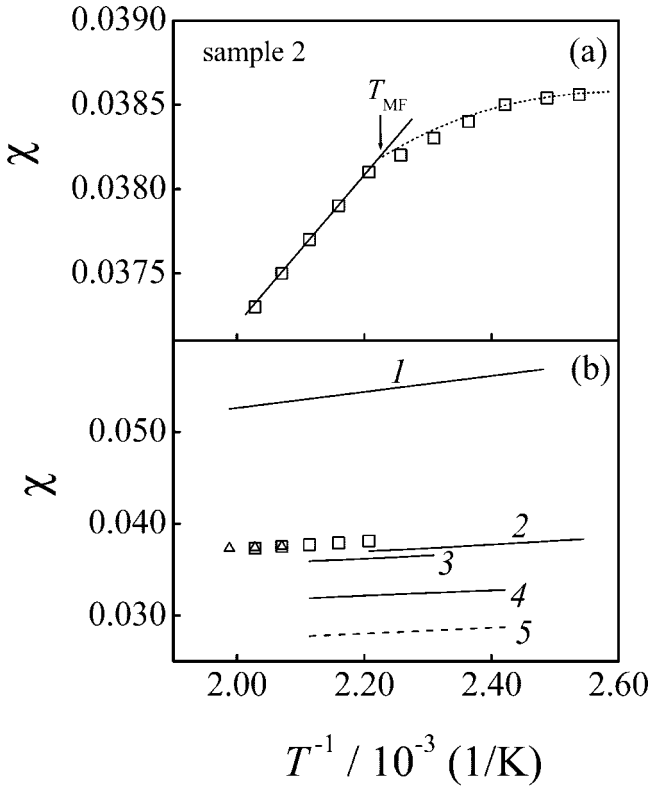

Figure 4. (a) Temperature dependence of χ for sample 2. The dotted line in the figure shows the leveling off in χ with T^{-1} below a crossover temperature denoted by T_{MF} from the mean-field theory (solid line). (b) Comparison of our experimental χ data (triangles for sample 1; squares for sample 2: $\chi = 0.0282 + 4.46/T$) to the literature reported data (line 1: [ref 17] PS-*b*-PMMA, $\chi = 0.035 + 8.8/T$; line 2: [refs 1 and 2] dPS-*b*-PMMA, $\chi = 0.0282 + 3.9/T$; line 3: [refs 1 and 2] PS-*b*-dPMMA, $\chi = 0.0292 + 3.2/T$; line 4: [refs 1 and 2] dPS-*b*-dPMMA, $\chi = 0.0251 + 3.2/T$; line 5: [ref 33] PS/PMMA, $\chi = 0.021 + 3.2/T$) from BCPs and blend systems, respectively.

for the effects of the molecular weight polydispersity and asymmetry in segmental volume. Detailed fitting information can be found in refs 19 and 20. Further details of specific equations and fitting parameters for our data analysis are provided as Supporting Information. Since the measurable temperature window of sample 2, where the sample is in a disordered state approximately characterized by the mean-field theory, is much wider than that of sample 1; sample 2 offers more reliable information on the temperature dependence of χ. The resultant χ values for sample 2 are shown in Figure 4a as a function of T^{-1}. We observe the crossover point, which is denoted by T_{MF} and marked by arrow. It is clearly shown that at $T > T_{MF}$ χ increases linearly with T^{-1}, but the increase of χ tends to level off at $T < T_{MF}$. This observation was extensively discussed in earlier publications.[19,29] The leveling off in χ at $T < T_{MF}$ in the disordered state indicates the deviation from the mean-field behavior such that concentration fluctuations having a large amplitude, large correlation length, and long lifetime predicted by the mean-field theory are suppressed by random thermal noise. The χ values extracted from the analyzed SAXS data at $T > T_{MF}$ can be written by

$$\chi = \chi_s + \chi_H/T \quad (1)$$

where χ_s and χ_H are the entropic and enthalpic contributions, respectively. The linear least-squares fit to the data for sample 2 at $T > T_{MF}$ yields

$$\chi = 0.0282 + 4.46/T \quad (2)$$

Our analysis shows that the entropic contribution, χ_s, to the net, χ, is much greater than the enthalpic contribution, χ_H/T, over the temperature range of our interest, leading to a weak temperature dependence of χ, a result consistent with the reports of Russell and co-workers for deuterated PS-*b*-PMMA systems.[1,2] Thus, a slight increase of the total number of segments in the PS-*b*-PMMA chains would lead to significant increase of the T_{ODT}.

We compare our results of χ values given by eq 2 to the literature data in Figure 4b. Line 1 represents $\chi = 0.035 + 8.8/T$ (Stühn, PS-*b*-PMMA sample in ref 17, $M_n \sim 13.3$K, $f_{PS} = 0.49$), which is much higher than other samples. Lines 2−4 are obtained from the labeled samples in ref 2, where line 2 represents $\chi = 0.0282 + 3.9/T$ (dPS-*b*-PMMA sample, $M_n \sim 27.7$K, $f_{d\text{-}PS} = 0.44$), line 3 represents $\chi = 0.0292 + 3.2/T$ (PS-*b*-dPMMA sample, $M_n \sim 27$ K, $f_{PS} = 0.50$), and line 4 represents $\chi = 0.0251 + 3.2/T$ (dPS-*b*-dPMMA sample, $M_n \sim 32.6$K, $f_{d\text{-}PS} = 0.48$). It is notable that these deuterated samples have similar molecular weights and compositions as our samples. At a given temperature, the χ value for our samples (shown as symbols in the figure) is a little bit larger than that of the labeled systems. On the other hand, Callaghan et al. reported an even lower χ value (line 5: PS/PMMA, $\chi = 0.021 + 3.2/T$) on the basis of cloud point measurements from homopolymer blends of PS and PMMA.[33]

Molecular weight effects and the role of architecture (block copolymer vs homopolymer) are thought to influence the averaged χ parameter in a system.[9] This is through contributions (of the order of $\sim 1/N$) from the different chain end and block copolymer junction chemistries. It is often difficult to find consistency between the experimental results of different groups. This is the case here where the results of Stühn et al.[17] are very different to our own and also to the values of Russell et al. and Callaghan et al. Our rationalization is that the differences are due to the lower molecular weights used by Stühn et al. Notably, Stühn et al. and Callaghan et al., both studying nondeuterated PS/PMMA systems, extracted χ parameters that are higher or lower than the values determined by Russell et al. The comparison of Callaghan et al. and Russell et al. results appears to indicate that a hydrogenated PS has a greater wetting power on a PMMA interface than its deuterated equivalent. This is inconsistent with a recent work of Harton et al., where dPS was shown to have a lower interaction energy with PMMA than PS.[12] Our own data support this conclusion.

In principle, the experimentally determined T_{ODT} and the experimentally derived χ parameter can be related by existing theory. Leibler determined a critical value of $\chi N = 10.5$ for phase separation, under the assumption of mean field and a monodisperse symmetric BCP system (of infinite N). Fredrickson and Helfand later predicted that fluctuations would increase the critical value of χN (with a correction as $N^{-1/3}$) and alter the transition to one that is weakly first order. This is the transition observed with SAXS. Therefore, the mean-field determined T_{ODT} should be higher than the experimentally observed T_{ODT}. Experimental work by Lynd and Hillmyer shows that polydispersity can stabilize an ordered phase against disorder (i.e., reduce the critical χN value).[34] It is easy to show that for the PS-*b*-PMMA system a change in N of a single segment alters the calculated T_{ODT} by ~7 °C. Given this sensitivity to N, arising from the insensitivity of the χ parameter to temperature, it is not reliable to make comparisons to the predictions of Leibler or Fredrickson and Helfand.

Conclusions

The order−disorder transition for two symmetric polystyrene-*b*-poly(methyl methacrylate) diblock copolymers was investigated by a high-temperature-resolution SAXS experiments with small decreases of T across the T_{ODT}. The characteristic T_{ODT} was determined experimentally from the discontinuity of I_m^{-1} and σ_q^2 vs T^{-1}. The discontinuity has not been reported so far for this particular BCP though the discontinuity has been reported for other BCPs. The results directly confirm the fluctuation-induced weakly first-order transition for this BCP also. In the disordered state, far above T_{ODT}, the χ parameter for PS-*b*-PMMA was also extracted and found to be slightly larger than that in the deuterated systems having the similar molecular weight and compositions. PS-*b*-PMMA is a promising technological system that is able to be manipulated to provide nanostructural templates and scaffolds.[35−38] Hence, our precise determination of χ and the order−disorder characteristics of a nondeuterated system will be invaluable to future works.

Acknowledgment. The authors acknowledge the funding provided by the Japan 21st Century Center of Excellence (COE) Program for a United Approach to New Materials at Kyoto University to participate in this research.

Supporting Information Available: SAXS scattering data analysis details. This material is available free of charge via the Internet at http://pubs.acs.org.

References and Notes

(1) Russell, T. P. *Macromolecules* **1993**, *26* (21), 5819–5819.
(2) Russell, T. P.; Hjelm, R. P.; Seeger, P. A. *Macromolecules* **1990**, *23* (3), 890–893.
(3) Hawker, C. J.; Russell, T. P. *MRS Bull.* **2005**, *30* (12), 952–966.
(4) Ruzette, A. V.; Leibler, L. *Nat. Mater.* **2005**, *4* (1), 19–31.
(5) Segalman, R. A. *Mater. Sci. Eng., R* **2005**, *48* (6), 191–226.
(6) Anastasiadis, S. H.; Russell, T. P.; Satija, S. K.; Majkrzak, C. F. *J. Chem. Phys.* **1990**, *92* (9), 5677–5691.
(7) Benoit, H.; Wu, W.; Benmouna, M.; Mozer, B.; Bauer, B.; Lapp, A. *Macromolecules* **1985**, *18* (5), 986–993.
(8) Bucknall, D. G. *Prog. Mater. Sci.* **2004**, *49* (5), 713–786.
(9) Dudowicz, J.; Freed, K. F. *Macromolecules* **1993**, *26* (1), 213–220.
(10) Fernandez, M. L.; Higgins, J. S.; Penfold, J.; Ward, R. C.; Shackleton, C.; Walsh, D. J. *Polymer* **1988**, *29* (11), 1923–1928.
(11) Fukuda, T.; Inagaki, H. *Pure Appl. Chem.* **1983**, *55* (10), 1541–1551.
(12) Harton, S. E.; Stevie, F. A.; Ade, H. *Macromolecules* **2006**, *39* (4), 1639–1645.
(13) Higgins, A. M.; Sferrazza, M.; Jones, R. A. L.; Jukes, P. C.; Sharp, J. S.; Dryden, L. E.; Webster, J. *Eur. Phys. J. E* **2002**, *8* (2), 137–143.
(14) Menelle, A.; Russell, T. P.; Anastasiadis, S. H.; Satija, S. K.; Majkrzak, C. F. *Phys. Rev. Lett.* **1992**, *68* (1), 67–70.
(15) Sivaniah, E.; Matsubara, S.; Zhao, Y.; Hashimoto, T.; Fukunaga, K.; Kramer, E. J.; Mates, T. E. *Macromolecules* **2008**, *41* (7), 2584–2592.
(16) Su, A. C.; Fried, J. R. *Macromolecules* **1986**, *19* (5), 1417–1421.
(17) Stühn, B. *J. Polym. Sci., Part B: Polym. Phys.* **1992**, *30* (9), 1013–1019.
(18) Stühn, B.; Mutter, R.; Albrecht, T. *Europhys. Lett.* **1992**, *18* (5), 427–432.
(19) Sakamoto, N.; Hashimoto, T. *Macromolecules* **1995**, *28* (20), 6825–6834.
(20) Sakurai, S.; Mori, K.; Okawara, A.; Kimishima, K.; Hashimoto, T. *Macromolecules* **1992**, *25* (10), 2679–2691.
(21) Amundson, K.; Helfand, E.; Patel, S. S.; Quan, X.; Smith, S. D. *Macromolecules* **1992**, *25* (7), 1935–1940.
(22) Wang, J. Y.; Chen, W.; Sievert, J. D.; Russell, T. P. *Langmuir* **2008**, *24* (7), 3545–3550.
(23) Brazovskii, S. A. *Zh. Eksp. Teor. Fiz.* **1975**, *68* (1), 175–185.
(24) Fredrickson, G. H.; Helfand, E. *J. Chem. Phys.* **1987**, *87* (1), 697–705.
(25) Leibler, L. *Macromolecules* **1980**, *13* (6), 1602–1617.
(26) Hashimoto, T.; Suehiro, S.; Shibayama, M.; Saijo, K.; Kawai, H. *Polym. J.* **1981**, *13* (5), 501–516.
(27) Hashimoto, T.; Todo, A.; Itoi, H.; Kawai, H. *Macromolecules* **1977**, *10* (2), 377–384.
(28) Todo, A.; Hashimoto, T.; Kawai, H. *J. Appl. Crystallogr.* **1978**, *11* (Oct), 558–563.
(29) Bates, F. S.; Rosedale, J. H.; Fredrickson, G. H. *J. Chem. Phys.* **1990**, *92* (10), 6255–6270.
(30) Floudas, G.; Pakula, T.; Fischer, E. W.; Hadjichristidis, N.; Pispas, S. *Acta Polym.* **1994**, *45* (3), 176–181.
(31) Hashimoto, T.; Ogawa, T.; Han, C. D. *J. Phys. Soc. Jpn.* **1994**, *63* (6), 2206–2214.
(32) Wolff, T.; Burger, C.; Ruland, W. *Macromolecules* **1993**, *26* (7), 1707–1711.
(33) Callaghan, T. A.; Paul, D. R. *Macromolecules* **1993**, *26* (10), 2439–2450.
(34) Lynd, N. A.; Hillmyer, M. A. *Macromolecules* **2007**, *40*, 8050–8055.
(35) Mansky, P.; Russell, T. P.; Hawker, C. J.; Pitsikalis, M.; Mays, J. *Macromolecules* **1997**, *30* (22), 6810–6813.
(36) Mizokuro, T.; Mochizuki, H.; Kobayashi, A.; Horiuchi, S.; Yamamoto, N.; Tanigaki, N.; Hiraga, T. *Chem. Mater.* **2004**, *16* (18), 3469–3475.
(37) Ruiz, R.; Sandstrom, R. L.; Black, C. T. *Adv. Mater.* **2007**, *19* (4), 587.
(38) Weng, C. C.; Wei, K. H. *Chem. Mater.* **2003**, *15* (15), 2936–2941.

MA8013004